# Self-Assembled Nanomaterials Using Magnetic Nanoparticles Modified with Polystyrene Brushes and Poly(styrene-*b*-butadiene-*b*-styrene)

**Ignacio García, Agnieszka Tercjak, Lorena Rueda, and Iñaki Mondragon***

*Materials and Technologies Group, Dpto. Ingeniería Química y M. Ambiente, Escuela Politécnica, University of the Basque Country, Pza Europa, 1, 20018 Donostia-San Sebastián, Spain*

*Received July 28, 2008; Revised Manuscript Received September 30, 2008*

ABSTRACT: Magnetic nanoparticles were studied to generate novel nanocomposites which maintain both magnetic properties of nanoparticles and self-assembly of amorphous block copolymer matrix. With this goal, iron oxide magnetic nanoparticles were modified with polystyrene (PS) brushes by atomic transfer radical polymerization (ATRP) to improve both the dispersion and the affinity of nanoparticles with one of the blocks of polystyrene-*b*-polybutadiene-*b*-polystyrene block copolymer. This way of preparation of nanocomposites opens new strategy to the generation of magnetic nanocomposites. The samples were characterized with the use of differential scanning calorimetry (DSC), dynamic mechanical analysis (DMA), rheological measurements, and atomic force microscopy (AFM).

## Introduction

Nanocomposites consisting of polymeric matrix and natural or synthetic layered minerals can be prepared by adjusting the interaction enthalpy between all components using specific compatibilization agents for the two intrinsically nonmiscible materials.[1] Polymer materials have been filled with several inorganic compounds to increase properties like heat resistance,[2] mechanical strength,[3] and impact resistance[4] or to decrease the permeability for gases like oxygen or water vapor.[5] The resulting materials must be seen as filled polymers because there is no or only little interaction between the two mixed components. These filled materials mostly lack from an intense interaction at the interface between the two partners. In general, macroscopic reinforcing elements contain always imperfections. Structural perfection is more and more reached if the reinforcing elements become smaller and smaller.[6] However, the smaller the reinforcing elements are, the larger is their external surface area and hence their tendency to agglomerate rather than to disperse homogenously in a matrix. Attempts to incorporate nanoparticles in a polymer matrix, in most of the cases due to the agglomeration tendency of the nanoparticles, has either been difficult to overcome or led to thermodynamically unstable mixtures.[7−11] In such systems, three components have to be considered: the surface of nanoparticles, the interface region, and the matrix polymer chains.[1] In general, it is necessary to adjust the thermodynamic interaction parameters of all components of the system. The resulting composites with surface modified nanoparticles display superior properties to those systems by simply mixing of components. In the case of ferromagnetic nanocomposites, the final properties closely depend on the size of nanoparticles and their state of dispersion and agglomeration.[12]

Nanocomposites can be an effective way to enhance mechanical and physical properties of polymers, but other properties such as transparency can be also modified. For nanocomposites, it is difficult to obtain a transparent film due to the need for mismatch of refractive index between the nanoparticles and the polymer matrix.[13−15] When a high light transmittance is needed, fine dispersion and small size of nanoparticles are of utmost importance.

* To whom all correspondence should be addressed: E-mail: inaki.mondragon@ehu.es.

Magnetic nanoparticle-based composites are receiving a growing interest for both technological and theoretical reasons, especially in the context of magnetic recording.[16]

Following our studies[17] about nanocomposites that contain magnetic nanoparticles modified with polystyrene brushes dispersed in amorphous polymer matrix as polystyrene-*b*-polybutadiene-*b*-polystyrene (SBS) triblock copolymer, in the present work these nanocomposites were characterized with the use of differential scanning calorimetry (DSC), dynamic mechanical analysis (DMA), rheological measurements, and atomic force microscopy (AFM).

## Experimental Section

**Materials.** Magnetite nanoparticles ($Fe_3O_4$; MN) were purchased from Integran Technologies Inc. (Canada). Polystyrene-*b*-polybutadiene-*b*-polystyrene (SBS) triblock copolymer (Dynasol C540) that contains 40 wt % polystyrene, was kindly gifted by Repsol-YPF. $M_n$ of PS and PB block is around 30000 and 45000 g/mol, respectively. Toluene was purchased from Fluka. The magnetic nanoparticles were modified with polystyrene (PS) brushes that were grown onto surface of MN (PS-MN) by atomic transfer radical polymerization (ATRP) as was shown in our previous work.[18]

**Preparation of Samples.** Nanocomposites were prepared by casting onto glass wafers using toluene solutions of 5 wt % SBS containing different percentages of inorganic material with respect to SBS. Samples of neat block copolymer and nanocomposites containing 1 and 2 wt % nanoparticles were annealed at 102 °C under vacuum and nanocomposites containing 4 wt % nanoparticles were annealed at 120 °C under vacuum.

**Experimental Techniques.** The rheological analysis was carried out in ARES rheometer (*Advanced Rheometrics Expansion System*, TA Instruments), equipped with a parallel plate geometry (diameters of 50 and 25 mm for the upper and lower plates, respectively) and two transductors, operating in the range of 0.02−200 g·cm and 2−2000 g·cm, depending on the generated torque values. Frequency sweeps were carried out at 120 °C over a frequency range of 0.004−100 rad/s and strain of 1%. Dynamic isochronal temperature and time scans were performed at a frequency of 6.28 rad/s. For temperature scans, the temperature range varied from 50 to 200 °C and heating rate was 5 °C $min^{-1}$. Then the upper plate was placed assuring that the normal strength was near zero to reach a thickness of about 1 mm and a sample diameter of 10 mm. The evolution of both storage ($G'$) and loss ($G''$) moduli was monitored upon frequency sweep. Storage and loss moduli were

10.1021/ma801701k CCC: $40.75 
Published on Web 11/06/2008

**Table 1. Glass Transition Temperatures**[a]

| | 1 wt % | | 2 wt % | | 3 wt % | |
|---|---|---|---|---|---|---|
| MN | −82[1] | 73[2] | −83[1] | 76[2] | −83[1] | 63[2] |
| PS-MN | −72[1] | 82/103[2] | −72[1] | 76/100[2] | −71[1] | 77/103[2] |

[a] Measured by DMA[1] and DSC[2], of nanocomposites containing different amounts of MN and PS-MN.

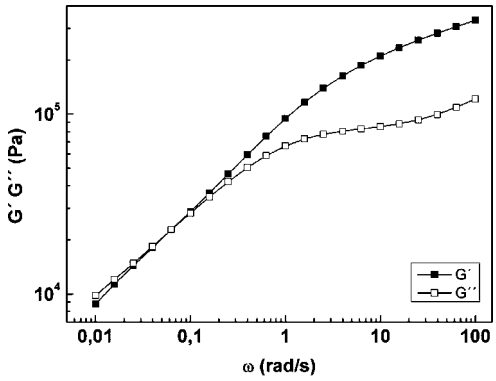


**Figure 1.** Frequency dependence of storage and loss moduli at 120 °C of SBS block copolymer.

calculated from the resulting torque values, being $\omega$ the frequency (rad/s), related to $f$ as $f$ (Hz) $= 2\pi\omega$ (rad/s).

Dynamic mechanical analysis was carried out using a Perkin-Elmer DMA7. The scans were carried out at a frequency of 1 Hz and a range of temperature between −100 and 25 °C with a heating rate of 5 °C/min. During the scans, the samples were subjected to a static force of 110 and a dynamic force of 100 mN.

Calorimetric measurements were performed in a Mettler Toledo DSC 822 differential scanning calorimeter equipped with a Sample Robot TSO 801 RO. Nitrogen was used as a purge gas (10 mL $min^{-1}$). Temperature and enthalpy were calibrated by using an indium standard. Measurements were performed in sealed aluminum pans containing a sample weight of around 10 mg with a range of temperature between 25 and 180 °C and heating rate was 10 °C $min^{-1}$.

Atomic force microscopy images were obtained in tapping mode with a scanning probe microscope (Nanoscope IIIa Multimode, Digital Instruments) equipped with an integrated phosphorus doped tip/cantilever having a resonance frequency of approximately 300 kHz and a spring constant of about 3 N/m; the tip radius was lower than 10 nm. Images show in the left part the surface morphology and in the right part the simultaneously taken phase image. An analysis of the AFM images was performed with WSxM software (Nanotec Electronica).

## Results and Discussion

The neat block copolymer and nanocomposites were characterized by DSC. Table 1 shows values of glass transition temperature ($T_g$) of nanocomposites that contain MN and PS-MN. The $T_g$ of polybutadiene was measured by DMA and $T_g$ of PS by DSC. In neat SBS, the $T_g$ of PB and polystyrene appear at −69 and 81 °C, respectively.[17] Several behaviors have been observed when nanocomposites have been analyzed by DSC. One of the cases is an increase in glass transition temperature of a nanocomposite due to reduction of polymer mobility.[19−21] In another hand, other authors have shown suppression of the thermal motion of the polymer chains when they contain well-dispersed inorganic material.[22]

When the $T_g$ values of PB and PS of nanocomposites that contain unmodified nanoparticles are compared, a diminution of both $T_g$ can be observed for MN/SBS nanocomposites as MN content increases. A decrease in $T_g$ of a nanocomposite can result from the increase of polymer mobility as a consequence of both bad dispersion and bad interfacial adhesion

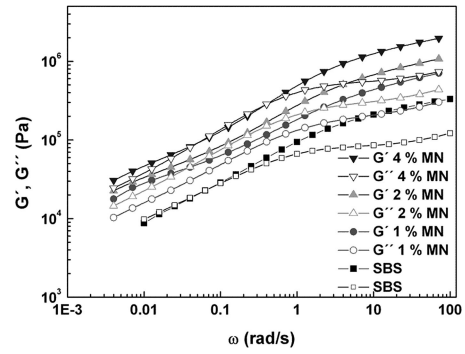


**Figure 2.** Frequency dependence of storage and loss moduli at 120 °C for nanocomposites containing different amounts of unmodified magnetic nanoparticles.

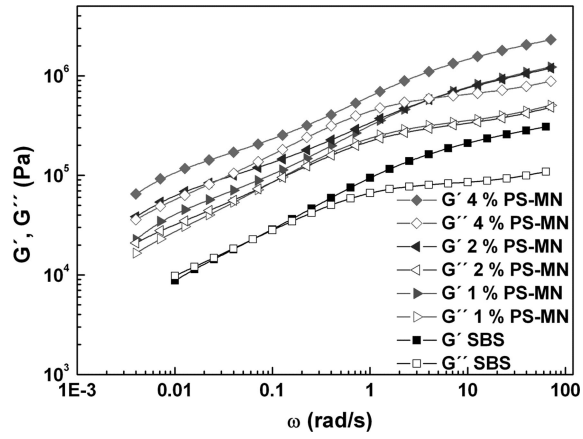


**Figure 3.** Frequency dependence of storage and loss moduli at 120 °C of nanocomposites that contain different amounts of modified magnetic nanoparticles.

between nanoparticles and polymer matrix. In the nanocomposites that contain PS-MN, by changing the quantity of nanoparticles, a nearly constant value of $T_g$ of PB can be observed around −71 °C. On the other hand, changes in $T_g$ of PS when the quantity of PS-MN is increased can be observed. The $T_g$ of PS of the nanocomposite that contains 1 wt % PS-MN indicates that PS-MN are in the PS phase of block copolymer due to the presence of two glass transition temperatures of PS, one related to PS domains without PS-MN and the other to PS domains that contain PS-MN, at around 82 and 103 °C,[17] respectively. It indicates that there are sites in the block copolymer without PS-MN and sites where PS-MN are confined on PS phase of the block copolymer, thus reducing the mobility of PS chains. Several authors[19−21] have shown that an increase in glass transition temperature of a nanocomposite results due to reduction of polymer mobility as a consequence of both fine dispersion and good interfacial adhesion between nanoparticles and PS phase of nanoparticles into polymer matrix. Same behavior, but slightly different values of $T_g$, in nanocomposite that contain 2 and 4 wt % of PS-MN can be observed. In these two cases, also, two $T_g$ for 2 wt % (around 76 and 100 °C) and 4 wt % (around 77 and 102 °C) can be observed for the PS domains. Due to the diminution of mobility of polymer chains when nanoparticles are introduced in block copolymer, the annealing temperature was increased from 102 to 120 °C for nanocomposites that contain 4 wt % of nanoparticles.

To know the rheological behavior of pure block copolymer, frequency sweeps from 0.004 rad/s to 100 rad/s at 120 °C were performed. Frequency sweeps were carried out after annealing under vacuum at 120 °C, that is a temperature above glass transition of PS. Figure 1 shows the frequency dependence of

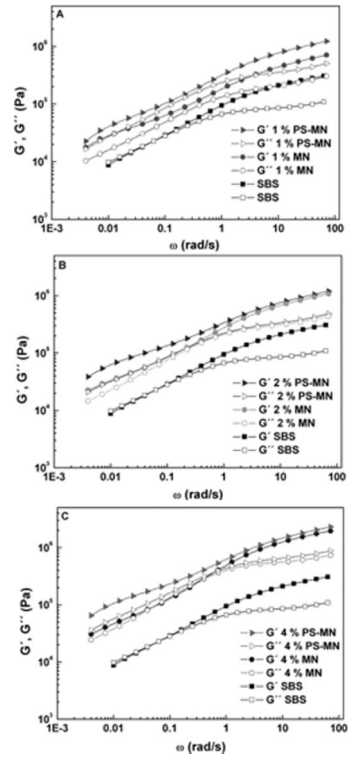


**Figure 4.** Storage and loss modulus as a function of frequency for neat block copolymer and nanocomposite with 1.0, 2.0, and 4.0 wt. % unmodified nanoparticles and nanoparticles modified with PS brushes. All measurements were carried out at 120 °C.

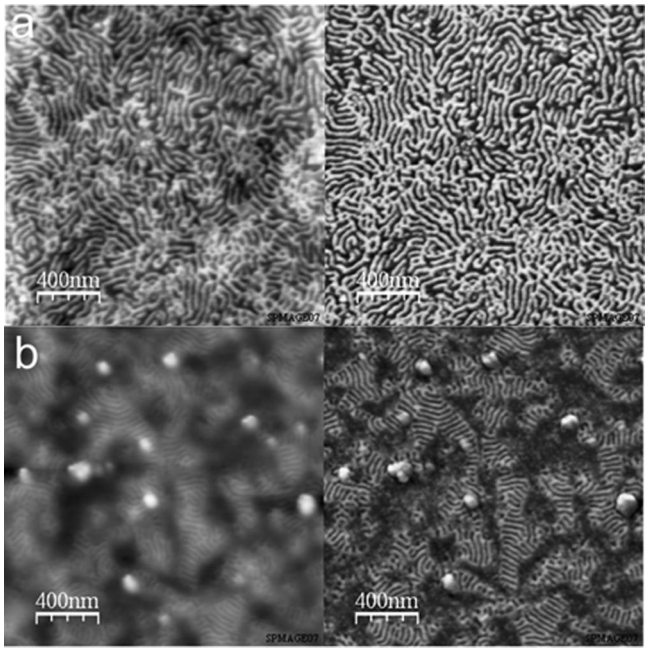


**Figure 5.** Representative tapping mode atomic force microscopy images for nanocomposite containing 2 wt % PS-MN (a) or MN (b) after annealing.

storage and loss moduli at 120 °C. At low frequencies, $G'$ and $G''$ are adequately represented by $\omega^{\alpha}$, where $\alpha \sim 0.5$. This value of $\alpha$ is attributed to the viscoelastic response of a lamellar microstructre.

Similar procedure was followed with nanocomposites that contain 1, 2, and 4 wt % MN (Figure 2) and PS-MN (Figure 3). In both cases, the frequency sweep spectra revealed that the addition of unmodified and modified nanoparticles lead to

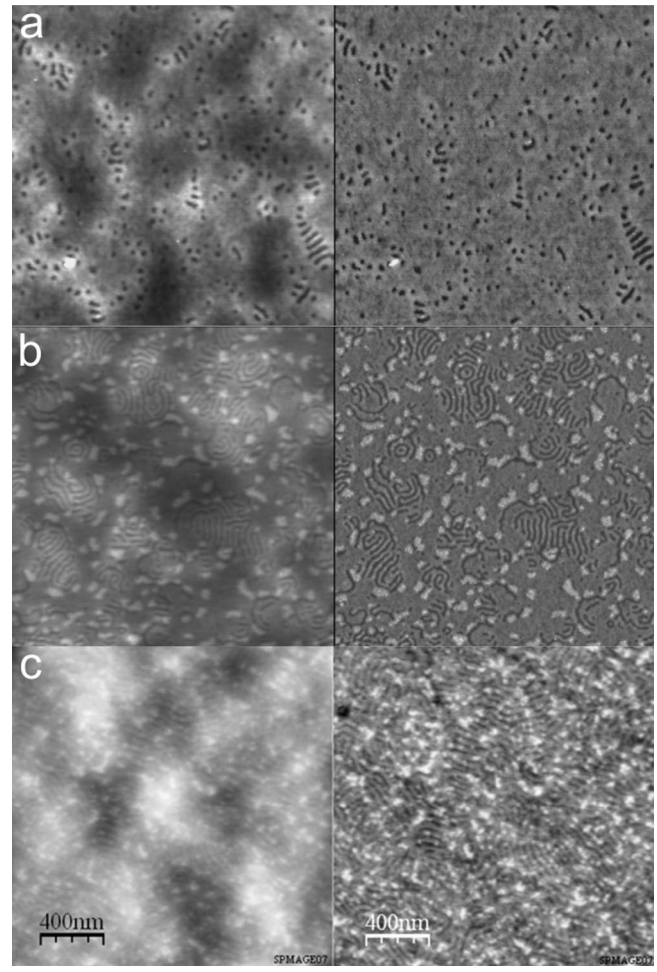


**Figure 6.** TM-AFM topography (left) and phase (right) images of film of nanocomposite containing 4 wt % PS-MN after 7 (a), 14 (b), and 24 h (c) annealing at 120 °C under vacuum.

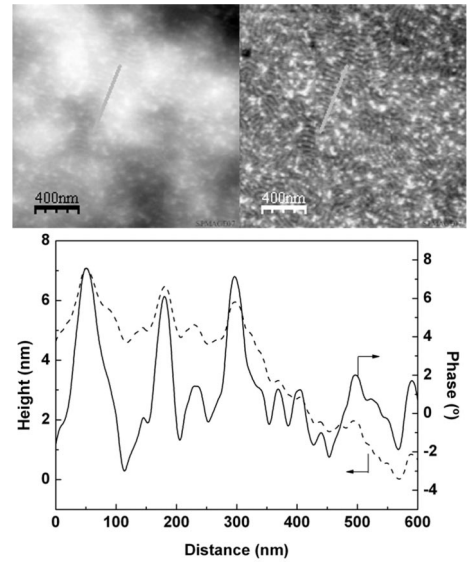


**Figure 7.** AFM images of SBS/4 wt % PS-MN nanocomposite: topography (left), phase (right), and corresponding height and phase profiles.

enhanced mechanical properties as both $G'$ and $G''$ increased as higher MN or PS-MN content was. The enhancement of modulus in all cases of nanocomposites of MN and PS-MN, when nanoparticles are aggregated, attributed to the addition of rigid nanoparticles.[23−25]

Figure 4a−c shows $G'$ and $G''$ of pure SBS, block copolymer containing 1, 2, and 4 wt % MN and PS-MN. Nanocomposites containing PS-MN presented a higher modulus than nanocomposites that contained MN. The fact that nanocomposites with PS-MN enhance mechanical properties more than nanocomposites with MN can be attributed to better interactions between PS-MN and PS microphase of SBS. In case of MN, the polymer chains of SBS that were able to intercalate between MN are not enough to avoid interactions between MN. As a consequence, the rise of the formation of aggregates would cause the diminution of storage modulus with respect to that for nanocomposites containing PS-MN.

Representative atomic force microscopy images for nanocomposite that contains 2 wt % PS-MN after annealing at 120 °C under vacuum are shown in Figure 5a. In these images, a lamellar microphase separation can be observed. Neither agglomerates nor aggregates of PS-MN can be observed, which is indicative of good distribution and dispersion of PS-MN inside the block copolymer matrix. Figure 5b shows lamellar microphase separation of nanocomposite that contains 2 wt % PS-MN after annealing. Aggregates of MN of diameter around 100 nm that are more or less uniformly dispersed can be observed. This good distribution and size of aggregates allows to increase the mechanical properties of nanocomposites with respect to the block copolymer, as shown in Figure 4. These AFM images allow to corroborate the results obtained by DSC and rheology.

Time evolution of nanostructure formation of nanocomposite that contains 4 wt % PS-MN is shown in Figure 6a−c. In AFM images, it is expected that PB appears dark and PS appears bright and nanoparticles are the brightest. First image shows nanocomposite after 7 h of annealing at 120 °C. Small microphase separated domains of polybutadiene can be observed. As seen in the second image, longer PB domains and some segregation of PS-MN seems to occur after 14 h of annealing. Last image shows the lamellar morphology of nanocomposite after 24 h of annealing. A deformed structure due to the incorporation and segregation of nanoparticles can be observed. DSC and rheology measurements were supported by these AFM images.

Nanocomposite containing 4 wt % PS-MN has a similar lamellar microstructure to neat block copolymer,[17] as can be observed in Figure 7. Two indicators allow to conclude that PS-MN were assembled into PS-block microphase separated domains of block copolymer. The first one is the very pronounced phase shift and the second is the increase of thickness of lamellae that distortions the morphology, both confirming that PS-MN were incorporated into PS block domains. To verify this behavior, phase profiles of nanocomposites have been studied. There is a correspondence between sizes of lamellae and intensity of phase. When the height of phase intensity is analyzed, an increase in the size of lamellae can be seen, the size of lamellae shows different values but they are always bigger than those for the neat block copolymer. This size variation can be attributed to confinement of nanoparticles inside polystyrene domains. The size variation originated because the nanoparticles did not completely fill the polystyrene domains. In the phase profile of nanocomposites, a variation in intensity across the profile can be observed. The higher intensity values can be attributed to sites where the PS-MN are inside of the polystyrene phase.

## Conclusions

A new technique for the preparation of amorphous nanocomposites based on magnetic nanoparticles embedded in SBS block copolymer has been proposed. This technique can open a new way on the generation of magnetic nanomaterials. One of the most important problems to obtain a good dispersion and confinement of inorganic materials inside a block copolymer has been solved by modification of commercial iron oxide nanoparticles with PS brushes grown by ATRP. SBS block copolymer which is able to self-assemble in lamellar morphology was used as matrix. The modification onto surface of nanoparticles allowed achieving their segregation inside PS phase.

The addition of unmodified nanoparticles increases both storage and loss moduli with respect to the neat block copolymer but the addition of magnetic nanoparticles anchored with PS brushes increases even more these properties. It is due to better interactions between PS-MN and PS domains of poly(styrene-b-butadiene-styrene) matrix. Polystyrene segmental motion decreases due to loss of mobility of this block as consequence of confinement of modified nanoparticles inside it.

Even if the morphology of nanocomposites did not change when compared with neat block copolymer, broader lamellaes were observed. This fact corresponds to nanoparticles were confined into PS domains of the block copolymer.

## References and Notes

(1) Fischer, H. *Mater. Sci. Eng., C* **2003**, *23*, 763.
(2) Brown, J. M.; Curliss, D.; Vaia, R. A. *Chem. Mater.* **2000**, *12*, 3376.
(3) Lim, S. T.; Hyun, Y. H.; Choi, H. J. *Chem. Mater.* **2002**, *14*, 1839.
(4) Vaia, R. A.; Maguire, J. F. *Chem. Mater.* **2007**, *19*, 2736.
(5) Merkel, T. C.; Freeman, B. D.; Spontak, R. J.; He, Z.; Pinnau, I.; Meakin, P.; Hill, A. J. *Chem. Mater.* **2003**, *15*, 109.
(6) Starkova, O.; Yang, J.; Zhang, Z. *Compos. Sci. Technol.* **2007**, *67*, 2691.
(7) Zhao, B. A. *Langmuir* **2004**, *20*, 11748.
(8) Devaux, C.; Chapel, J. P.; Chaumont, Ph. *Eur. Phys. J. E* **2002**, *7*, 345.
(9) Kasseh, A.; Ait-Kadi, A.; Riedl, B.; Pierson, J. F. *Polymer* **2003**, *44*, 1367.
(10) Ohno, K.; Koh, K.; Tsujii, Y.; Fukuda, T. *Macromolecules* **2002**, *35*, 8989.
(11) Matsuno, R.; Yamamoto, K.; Otsuka, H.; Takahara, A. *Macromolecules* **2004**, *37*, 2203.
(12) Jolivet, J.-P.; Tronc, E.; Chanéac, C. *C. R. Chim.* **2002**, *5*, 659.
(13) Li, Y.; Fu, S.; Yang, Y.; Mai, Y. *Chem. Mater.* **2008**, *20*, 2637.
(14) Yamasaki, T.; Tsutsui, T. *Appl. Phys. Lett.* **1998**, *72*, 1957.
(15) Gu, C.; Kubo, S.; Qian, W.; Einaga, Y.; Tryk, D. A.; Fujishima, A.; Satu, O. *Langmuir* **2001**, *17*, 6751.
(16) Jogo, A.; Nagasaka, K.; Ibusuki, T.; Shimizu, Y.; Tanaka, A.; Oshima, H. *J. Magn. Magn. Mater.* **2007**, *309*, 80.
(17) Garcia, I.; Tercjak, A.; Zafeiropoulos, N. E.; Stamm, M.; Mondragon, I. *Macromol. Rapid Commun.* **2007**, *28*, 2361.
(18) Garcia, I.; Tercjak, A.; Zafeiropoulos, N. E.; Stamm, M.; Mondragon, I. *J. Polym. Sci., Part A: Polym. Chem.* **2007**, *45*, 4744.
(19) Yeh, S. W.; Wei, K. H.; Sun, Y. S.; Jeng, U. S.; Liang, K. S. *Macromolecules* **2005**, *38*, 6559.
(20) Honga, R. Y.; Pana, T. T.; Li, H. Z. *J. Magn. Magn. Mater.* **2006**, *303*, 60.
(21) Kontou, E.; Niaounakis, M. *Polymer* **2006**, *47*, 1267.
(22) Podsiadlo, P.; Kaushik, A. M.; Arruda, E. M.; Waas, A. M.; Shim, B. S.; Xu, J.; Nandivana, H.; Pumplin, B. J.; Lahann, J.; Ramamoorthy, A.; Kotov, N. A. *Science* **2007**, *318*, 80.
(23) Wook., D.; Chul, B. *Polym. Adv. Technol.* **2005**, *16*, 846.
(24) Kotsilkova, R.; Nesheva, D.; Nedkov, I.; Krusteva, E.; Stavrev, S. *J. Appl. Polym. Sci.* **2004**, *92*, 2220.
(25) Pattanayak, A.; Jana, S. C. *Polymer* **2005**, *46*, 3394.

MA801701K